

Chapter 2

Applications of the Plate Membrane Theory

In this chapter we will give solutions for plates, which are loaded only on their edges. This implies that no distributed forces p_x and p_y occur, and the fourth-order bi-harmonic equation (1.23) reduces to the simple form

$$\nabla^2 \nabla^2 u_x = 0 \quad (2.1)$$

When a general solution has been found for u_x , the solution for u_y can be derived from the relation between u_x and u_y as given in Eq. (1.17). If we choose the first equation, the relation is ($p_x = p_y = 0$)

$$\left(\frac{\partial^2}{\partial x^2} + \frac{1-\nu}{2} \frac{\partial^2}{\partial y^2} \right) u_x + \left(\frac{1+\nu}{2} \frac{\partial^2}{\partial x \partial y} \right) u_y = 0 \quad (2.2)$$

We will demonstrate two types of solution. In the first type, solutions for the displacements u_x and u_y will be tried, which are polynomials in x and y . We will see that interesting problems can be solved through this ‘inverse method’. The second type of solution is found by assuming a periodic distribution (sine or cosine) in one direction. Then in the other direction an ordinary differential equation has to be solved. This approach is suitable for deep beams or walls.

2.1 Trial Solutions in the Form of Polynomials

In this section we consider problems of which we know the stress state. For this stress state we want to determine the displacement field. For this purpose

appropriate trial functions for the displacements u_x and u_y will be chosen, in which a number of coefficients occur, yet to be determined. As a trial solution in its most general form we can choose

$$u_x(x, y) = a_1 + a_2x + a_3y + a_4x^2 + a_5xy + a_6y^2 + a_7x^3 + a_8x^2y + a_9xy^2 + a_{10}y^3 + a_{11}x^3y + a_{12}xy^3 \quad (2.3)$$

$$u_y(x, y) = b_1 + b_2x + b_3y + b_4x^2 + b_5xy + b_6y^2 + b_7x^3 + b_8x^2y + b_9xy^2 + b_{10}y^3 + b_{11}x^3y + b_{12}xy^3 \quad (2.4)$$

All 12 polynomial terms in Eq. (2.3) for u_x are independent solutions of the differential equation (2.1), so the 12 coefficients a_i are independent of each other. In the same way is Eq. (2.4) a general solution for the bi-harmonic equation for u_y .

In this section we start with the simple case that only constant and linear polynomial terms are chosen. After that a problem is solved for which we have to consider quadratic terms. Finally a problem will be solved for which we also have to include cubic terms.

2.1.1 Homogeneous Stress States

We consider the constant and linear terms with coefficients a_1, a_2, a_3, b_1, b_2 , and b_3

$$u_x(x, y) = a_1 + a_2x + a_3y; \quad u_y(x, y) = b_1 + b_2x + b_3y \quad (2.5)$$

Together the six terms determine all possible states of homogeneous strains and all possible rigid body displacements, as can easily be shown. Applying the kinematic relations (1.9) we find the strains

$$\left. \begin{aligned} \varepsilon_{xx} &= a_2 \\ \varepsilon_{yy} &= b_3 \\ \gamma_{xy} &= a_3 + b_2 \end{aligned} \right\} \quad \text{Homogeneous strains}$$

These strains are constant over the plate domain. The constants a_1 and b_1 do not appear in the strains at all. Those represent the rigid body translations. Of the constants a_3 and b_2 , only the sum appears in the strains. The difference of these constants defines a rigid body rotation. The three rigid body motions are

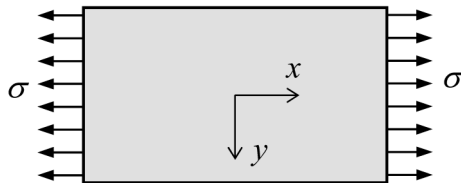


Figure 2.1 Constant tensile stress.

$$\left. \begin{aligned} u_x &= a_1 \\ u_y &= b_1 \\ \omega_{xy} &= \frac{1}{2}(-a_3 + b_2) \end{aligned} \right\} \text{Rigid body motions}$$

The homogenous strain state of Eq. (2.6) defines the stresses. From the constitutive law in Eq. (1.13) we find for $t = 1$

$$\begin{aligned} \sigma_{xx} &= \frac{E}{1 - \nu^2} (a_2 + \nu b_3) \\ \sigma_{yy} &= \frac{E}{1 - \nu^2} (b_3 + \nu a_2) \\ \sigma_{xy} &= \frac{E}{2(1 + \nu)} (a_3 + b_2) \end{aligned} \quad (2.8)$$

In the two following examples we will determine the three coefficients a_i and three coefficients b_i for some special cases.

Case 1: Constant Normal Stress

A plate of unit thickness will be analyzed; it is subjected to a constant (uniaxial) tensile stress σ in the x -direction (see Figure 2.1). The loads p_x and p_y are zero. We need six conditions to find the coefficients a_i and b_i . We know $\sigma_{xx} = \sigma$, $\sigma_{yy} = 0$, and $\sigma_{xy} = 0$, and we prescribe that no translations or rotations occur at the origin of the coordinate system. The stresses satisfy the equilibrium conditions in (1.14). Accounting for Eq. (2.8), we obtain three conditions for stresses

$$\frac{E}{1 - \nu^2} (a_2 + \nu b_3) = \sigma; \quad b_3 + \nu a_2 = 0; \quad a_3 + b_2 = 0 \quad (2.9)$$

Equation (2.7) for the rigid body motions specifies three other conditions:

$$a_1 = 0; \quad b_1 = 0; \quad -a_3 + b_2 = 0 \quad (2.10)$$

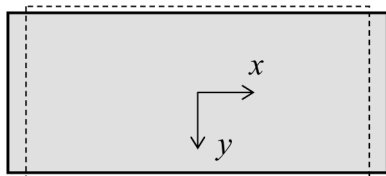


Figure 2.2 Deformation without zero rigid body motion.

These six equations imply

$$\begin{aligned} a_1 &= 0; & a_2 &= \frac{\sigma}{E}; & a_3 &= 0 \\ b_1 &= 0; & b_2 &= 0; & b_3 &= -\nu \frac{\sigma}{E} \end{aligned} \quad (2.11)$$

The displacement field equation (2.5) then becomes

$$u_x = \frac{\sigma}{E}x; \quad u_y = -\nu \frac{\sigma}{E}y \quad (2.12)$$

The middle of the plate does not translate or rotate. So the left-hand side of the plate moves towards the left, and the right-hand side towards the right (see Figure 2.2). In the lateral direction contraction takes place; this yields a negative displacement u_y for positive values y , and a positive displacement for negative values.

As an alternative we could have required the left-hand side not to move. In that case a rigid body displacement u_0 has to be added (a displacement of the plate towards the right as shown in Figure 2.3, and instead of $a_1 = 0$ we should choose $a_1 = u_0$.

Note

We have two states of equal stresses, but different displacement fields. The difference consists of rigid body motions.

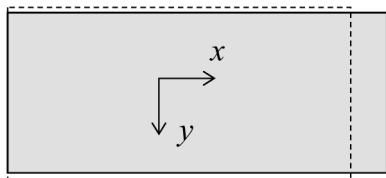


Figure 2.3 Deformation with rigid body motion in x -direction.

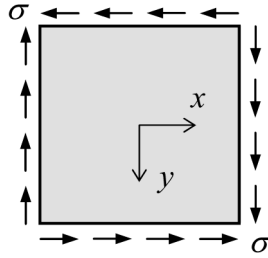


Figure 2.4 Constant shear stress.

Case 2: Constant Shear Stress

Consider a plate undergoing pure shear σ (see Figure 2.4). This stress state satisfies the equilibrium conditions in Eq. (1.14). We do not permit rigid body displacements a_1 and b_1 . However, we take into account a rigid body rotation ω . The stresses are, see Eq. (2.8)

$$a_2 + \nu b_3 = 0; \quad b_3 + \nu a_2 = 0; \quad \frac{E}{2(1 + \nu)}(a_3 + b_2) = \sigma \quad (2.13)$$

The rigid body displacements are, see Eq. (2.76)

$$a_1 = 0; \quad b_1 = 0; \quad \frac{1}{2}(-a_3 + b_2) = \omega \quad (2.14)$$

From Eqs. (2.13) and (2.14) we find four zero values

$$a_1 = 0; \quad a_2 = 0; \quad b_1 = 0; \quad b_3 = 0 \quad (2.15)$$

Only two equations remain with coefficients a_3 and b_2

$$\sigma = \frac{E}{2(1 + \nu)}(a_3 + b_2); \quad \omega = \frac{1}{2}(-a_3 + b_2) \quad (2.16)$$

Therefore the displacements will be

$$u_x = a_3 y; \quad u_y = b_2 x \quad (2.17)$$

Now, we will consider three subcases.

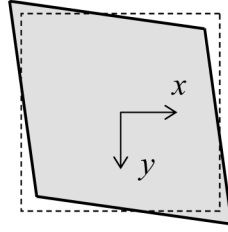


Figure 2.5 Deformation without rigid body rotation.

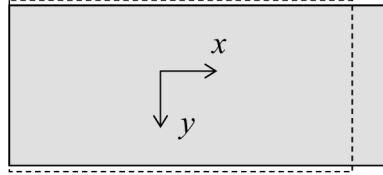


Figure 2.6 Deformation with rigid body motion in x -direction.

Subcase 2.1

No rigid body rotation (see Figure 2.5) occurs. We choose

$$\omega = 0 \rightarrow a_3 = b_2 = \frac{(1 + \nu)\sigma}{E} \quad (2.18)$$

and therefore

$$u_x = \frac{(1 + \nu)\sigma}{E}y; \quad u_y = \frac{(1 + \nu)\sigma}{E}x \quad (2.19)$$

The linear distribution of u_x in y -direction and of u_y in x -direction is confirmed by the deformation as shown in Figure 2.5.

Subcase 2.2

No displacement in x -direction (see Figure 2.6) takes place. The plate has vertical edges after a rigid body rotation. Now

$$a_3 = 0 \rightarrow b_2 = \frac{2(1 + \nu)\sigma}{E}; \quad \omega = \frac{(1 + \nu)\sigma}{E} \quad (2.20)$$

and therefore

$$u_x = 0; \quad u_y = \frac{2(1 + \nu)\sigma}{E}x \quad (2.21)$$

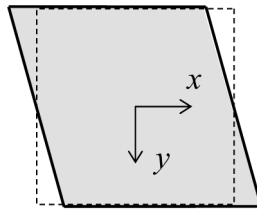


Figure 2.7 Deformation with zero displacement in y -direction.

Subcase 2.3

There is no displacement in the y -direction (see Figure 2.7). The plate has horizontal edges after a rigid body rotation. Now

$$b_2 = 0 \rightarrow a_3 = \frac{2(1+\nu)\sigma}{E}; \quad \omega = -\frac{(1+\nu)\sigma}{E} \quad (2.22)$$

and therefore

$$u_x = \frac{2(1+\nu)\sigma}{E}y; \quad u_y = 0 \quad (2.23)$$

Same Stress, Different Displacements

In all three cases the same shear stress occurs, however the displacement fields are different. The difference is related to the magnitude and sign of the rigid body rotation.

Case 3: Rigid Body Displacements

There is a field of displacements that consists only of rigid body displacements

$$\begin{aligned} u_x(x, y) &= C_1 - C_3 y \\ u_y(x, y) &= C_2 + C_3 x \end{aligned} \quad (2.24)$$

Substitution into the kinematic equations (1.9) shows that the three strains are zero. Therefore the three stresses will be zero too. The constants C_1 and C_2 relate to translations; the constant C_3 to rotation.

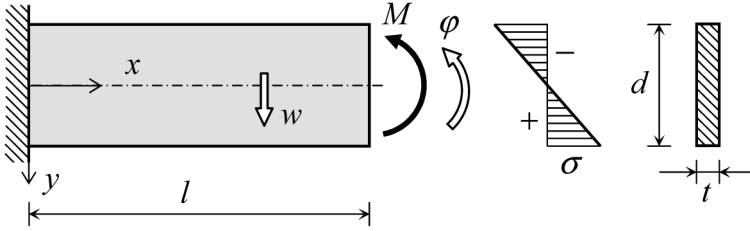


Figure 2.8 Cantilever beam subjected to pure bending.

2.1.2 Constant Bending Moment in Beam

Consider the classic Euler–Bernoulli beam theory [1] of a cantilever beam loaded by a moment at the free end, see Figure 2.8. In this case, no shear force V occurs, and the bending moment M is constant (and positive) over the length of the beam. In the beam theory the stresses in the beam are

$$\sigma_{xx} = \frac{M}{I}y; \quad \sigma_{yy} = 0; \quad \sigma_{xy} = 0 \quad (2.25)$$

Here $I = d t^3/12$ is the second moment of the cross-sectional area, where d is the width and t the depth of the beam. This stress distribution has been derived in classical beam theory on the assumption that a plane cross-section remains plane after applying the load. The stress state equation (2.25) satisfies the equilibrium conditions in (1.14) and therefore is a set of equilibrating stresses. In the stresses of Eq. (2.25) a term occurs which is linear in y , which means that we also can expect linear terms in the strains. Because strains are first derivatives of displacements, we therefore must consider quadratic displacement terms. We start with the most general form of all quadratic terms

$$u_x(x, y) = a_4x^2 + a_5xy + a_6y^2; \quad u_y(x, y) = b_4x^2 + b_5xy + b_6y^2 \quad (2.26)$$

The strains and stresses are now

$$\begin{aligned} \varepsilon_{xx} &= 2a_4x + a_5y \\ \varepsilon_{yy} &= b_5x + 2b_6y \\ \gamma_{xy} &= (a_5 + 2b_4)x + (2a_6 + b_5)y \end{aligned} \quad (2.27)$$

$$\begin{aligned}
\sigma_{xx} &= \frac{E}{1-\nu^2} \{ (2a_4 + \nu b_5)x + (a_5 + 2\nu b_6)y \} \\
\sigma_{yy} &= \frac{E}{1-\nu^2} \{ (2\nu a_4 + b_5)x + (\nu a_5 + 2b_6)y \} \\
\sigma_{xy} &= \frac{E}{2(1+\nu)} \{ (a_5 + 2b_4)x + (2a_6 + b_5)y \}
\end{aligned} \tag{2.28}$$

A comparison of these stresses with the actual stresses leads to six conditions

$$\begin{aligned}
2a_4 + \nu b_5 &= 0, & \nu a_5 + 2b_6 &= 0 \\
a_5 + 2b_4 &= 0, & \frac{E}{1-\nu^2} (a_5 + 2\nu b_6) &= \frac{M}{I} \\
2\nu a_4 + b_5 &= 0, & 2a_6 + b_5 &= 0
\end{aligned} \tag{2.29}$$

The solution of these six equations is

$$\begin{aligned}
a_4 &= 0; & a_5 &= \frac{M}{EI}; & a_6 &= 0 \\
b_4 &= -\frac{M}{2EI}; & b_5 &= 0; & b_6 &= -\frac{\nu M}{2EI}
\end{aligned} \tag{2.30}$$

Therefore the displacements are

$$u_x(x, y) = \frac{M}{EI}xy; \quad u_y(x, y) = -\frac{M}{2EI}(x^2 + \nu y^2) \tag{2.31}$$

For a homogenous moment distribution, the classical assumption that a plane cross-section remains plane after loading is correct, as appears from Eq. (2.31), because u_x has a linear dependence on y for each value of x . The stress state does not change when a rigid body displacement is added, as defined in Eq. (2.24). In total we get

$$\begin{aligned}
u_x(x, y) &= \frac{M}{EI}xy + c_1 - c_3y \\
u_y(x, y) &= -\frac{M}{2EI}(x^2 + \nu y^2) + c_2 + c_3x
\end{aligned} \tag{2.32}$$

The three constants c_1 , c_2 and c_3 have to be found from the boundary conditions. In the example we have a support in $x = 0$. We interpret this support as conditions that hold for $x = 0$, $y = 0$. The axis of the beam at $x = 0$ cannot translate and rotate, the bar axis remains horizontal.

$$\left. \begin{aligned} u_x &= 0; & u_y &= 0 \\ \frac{\partial u_y}{\partial x} &= 0 \end{aligned} \right\} \quad \text{for } x = 0, y = 0 \quad (2.33)$$

Substitution of Eq. (2.32) into Eq. (2.33) leads to

$$c_1 = 0; \quad c_2 = 0; \quad c_3 = 0 \quad (2.34)$$

Apparently the displacements in Eq. (2.32) already fully meet the boundary conditions. To interpret these results, we move over to the deflection w and the rotation φ of the cross-section. Because the section is plane after deformation we can write

$$u_x = y\varphi, \quad u_y = w \quad (2.35)$$

This changes Eq. (2.32) into

$$\varphi = \frac{M}{EI}x, \quad w = -\frac{1}{2} \frac{M}{EI}(x^2 + \nu y^2) \quad (2.36)$$

At the free end of the beam, at the position of the axis ($x = l, y = 0$), we find

$$\varphi = \frac{Ml}{EI}, \quad w = -\frac{1}{2} \frac{Ml^2}{EI} \quad (2.37)$$

These results are well known from elementary beam theory. The rotation φ is both the inclination of the beam axis and the tilt of the cross-section plane.

Check on Euler–Bernoulli beam theory

We conclude that the well known results of Euler–Bernoulli beam theory are confirmed by plate theory. From Eq. (2.36) it follows, that the rotation φ increases linearly with x and the vertical deflection w is square in x . In one way the results of the plane stress theory differ from Euler–Bernoulli beam theory. The predicted deflections are the same only along the axis of the beam, where $y = 0$. Outside the beam axis a small correction factor is needed when $\nu \neq 0$. So, strictly speaking, the assumption of the deflection on all points along the height of the beam being the same is incorrect. However, for slender beams the correction term is an order $\nu(d/l)^2$ smaller than the main term. This is of the order of 1% or less, so the assumption in the beam theory is acceptable.

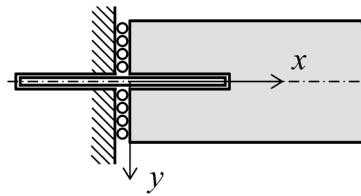


Figure 2.9 Detail of the boundary condition at the restrained end.

Remark

The boundary condition in $x = 0$, $y = 0$ in fact means that the horizontal displacement u_x is obstructed in the complete vertical cross-section in $x = 0$, but that the vertical displacement u_y could occur freely in this section, except for $y = 0$, see Figure 2.9. The bar axis is horizontal at the clamped end.

2.1.3 Constant Shear Force in Beam

We increase the complexity of the cantilever beam by replacing the moment at the free end by a downward vertical force F as shown in Figure 2.10. Now there is a constant shear force V (positive) and the bending moment M varies linearly along the beam axis (negative). The expressions for M and V are

$$M = F(x - l), \quad V = F \quad (2.38)$$

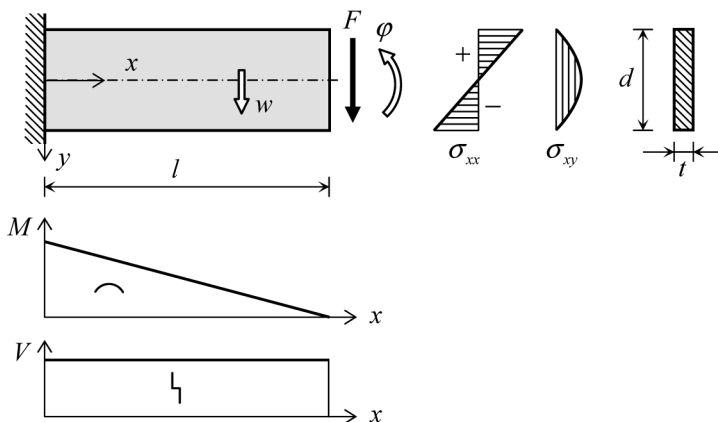


Figure 2.10 Cantilever beam loaded by point load.

The stresses are

$$\begin{aligned}\sigma_{xx} &= \frac{My}{I} = \frac{F}{I}(xy - ly) \\ \sigma_{yy} &= 0 \\ \sigma_{xy} &= \frac{3}{2} \left(1 - \frac{4y^2}{d^2}\right) \frac{V}{A} = \frac{3F}{2A} \left(1 - \frac{4y^2}{d^2}\right)\end{aligned}\quad (2.39)$$

where

$$A = td; \quad I = \frac{1}{12}td^3 \quad (2.40)$$

This set of equations satisfies the equilibrium equations in (1.14). The boundary conditions in the left end of the beam axis ($x = 0$, $y = 0$) are chosen in the same fashion as in the previous example with the moment load (horizontal bar axis)

$$u_x = 0; \quad u_y = 0; \quad \frac{\partial u_y}{\partial x} = 0 \quad (2.41)$$

In the expression for the stress σ_{xx} , a term $-Fly/I$ is present which we recognize as the distribution of a constant moment $M = -Fl$. For such a stress state we already found

$$u_x = \frac{M}{EI}xy = -\frac{Fl}{EI}xy; \quad u_y = \frac{1}{2} \frac{M}{EI}(x^2 + \nu y^2) = \frac{Fl}{2EI}(x^2 + \nu y^2) \quad (2.42)$$

In the stress σ_{xy} , a constant part $3F/2A$ is also present. Taking into account the boundary conditions, subcase 3 of case 2 (Section 2.1.1) is applicable. We substitute $G = E/2(1 + \nu)$

$$u_x = \frac{\sigma}{G}y = \frac{3F}{2GA}y, \quad u_y = 0 \quad (2.43)$$

The residual part of the stresses is

$$\sigma_{xx} = \frac{F}{I}xy; \quad \sigma_{yy} = 0; \quad \sigma_{xy} = -\frac{6F}{Ad^2}y^2 \quad (2.44)$$

The displacement field corresponding with these stresses still needs to be determined. Quadratic stress polynomials imply quadratic strain polynomials and cubic displacement polynomials, because strains are the first derivative of the displacements. So, we start from the most general cubic terms

$$\begin{aligned}u_x(x, y) &= a_7x^3 + a_8x^2y + a_9xy^2 + a_{10}y^3 \\ u_y(x, y) &= b_7x^3 + b_8x^2y + b_9xy^2 + b_{10}y^3\end{aligned}\quad (2.45)$$

The corresponding strains are

$$\begin{aligned}\varepsilon_{xx} &= 3a_7x^2 + 2a_8xy + a_9y^2 \\ \varepsilon_{yy} &= b_8x^2 + 2b_9xy + 3b_{10}y^2 \\ \gamma_{xy} &= (a_8 + 3b_7)x^2 + 2(a_9 + b_8)xy + (3a_{10} + b_9)y^2\end{aligned}\quad (2.46)$$

and the stresses

$$\begin{aligned}\sigma_{xx} &= \frac{E}{1-\nu^2} \{ (3a_7 + \nu b_8)x^2 + 2(a_8 + \nu b_9)xy + (a_9 + 3\nu b_{10})y^2 \} \\ \sigma_{yy} &= \frac{E}{1-\nu^2} \{ (3\nu a_7 + b_8)x^2 + 2(\nu a_8 + b_9)xy + (\nu a_9 + 3b_{10})y^2 \} \\ \sigma_{xy} &= \frac{E}{2(1+\nu)} \{ (a_8 + 3b_7)x^2 + 2(a_9 + b_8)xy + (3a_{10} + b_9)y^2 \}\end{aligned}\quad (2.47)$$

A comparison with Eq. (2.44) leads to the conditions

$$\begin{aligned}3a_7 + \nu b_8 &= 0, & \frac{2E}{1-\nu^2}(a_8 + \nu b_9) &= \frac{F}{I}, & a_9 + 3\nu b_{10} &= 0 \\ 3\nu a_7 + b_8 &= 0, & \nu a_8 + b_9 &= 0, & \nu a_9 + 3b_{10} &= 0 \\ a_8 + 3b_7 &= 0, & a_9 + b_8 &= 0, & G(3a_{10} + b_9) &= -\frac{6F}{Ad^2}\end{aligned}\quad (2.48)$$

The solution of these nine equations for eight unknown coefficients produces only four no-zero coefficients

$$a_8 = \frac{F}{2EI}, \quad a_{10} = \frac{\nu F}{6EI} - \frac{2F}{GA d^2}, \quad b_7 = -\frac{F}{6EI}, \quad b_9 = -\frac{\nu F}{2EI} \quad (2.49)$$

The displacements in this case have become

$$u_x = a_8x^2y + a_{10}y^3, \quad u_y = b_7x^3 + b_9xy^2 \quad (2.50)$$

Substitution of Eq. (2.49) leads to

$$\begin{aligned}u_x &= \frac{F}{2EI}x^2y + \left(\frac{\nu F}{6EI} - \frac{2F}{GA d^2} \right) y^3 \\ u_y &= -\frac{F}{6EI}x^3 - \frac{\nu F}{2EI}xy^2\end{aligned}\quad (2.51)$$

The total displacement field is found by adding Eqs. (2.42), (2.43) and (2.51), and the addition of a rigid body displacement. In this final result we assemble the terms with EI and the terms with GA and find

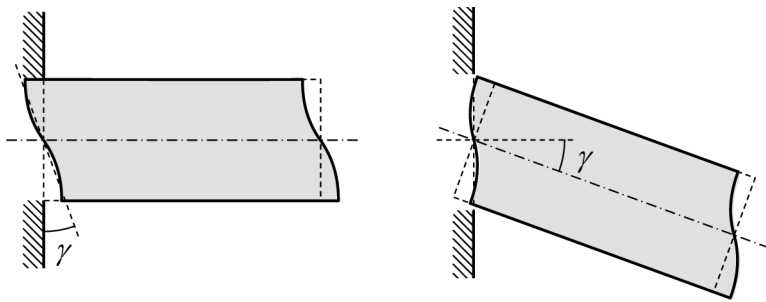


Figure 2.11 Rotation due to ‘mean’ shear deformation.

$$\begin{aligned}
 u_x &= \frac{F}{EI} \left\{ x \left(\frac{1}{2}x - l \right) y + \frac{\nu}{6} y^3 \right\} + \frac{F}{GA d^2} \left(-2y^3 + \frac{3}{2} d^2 y \right) + c_1 - c_3 y \\
 u_y &= \frac{F}{EI} \left\{ x^2 \left(-\frac{1}{6}x + \frac{1}{2}l \right) + \nu \left(-\frac{1}{2}x - \frac{1}{2}l \right) y^2 \right\} + c_2 + c_3 x
 \end{aligned} \tag{2.52}$$

The boundary conditions (2.41) are met for $c_1 = 0$, $c_2 = 0$, $c_3 = 0$. If we define the rotation φ as the inclination of the beam axis

$$\varphi = -\frac{\partial u_y}{\partial x} \tag{2.53}$$

and the displacement w as the vertical displacement u_y of the beam axis, the rotation φ and deflection w of the free beam end (in the axis of the beam) are

$$\varphi = -\frac{1}{2} \frac{F l^2}{EI}, \quad w = \frac{1}{3} \frac{F l^3}{EI} \tag{2.54}$$

Again, these are equal to the well-known results of classical beam theory. However, the cross-sections no longer remain plane. In u_x , not only linear terms in y are present, but also terms y^3 , even when $\nu = 0$. Nonetheless, the bending stress develops linearly over the height of the beam. So, an erroneous assumption in classical beam theory has led in the past to correct solutions for the stresses!

Now we want to have a closer look at the shape of the deformed beam at the restrained end (see the left figure of Figure 2.11). We see that a horizontal beam axis does not imply that the cross-section takes up a vertical position. First, the cross-section is distorted. In addition, the ‘mean’ cross-section is tilted. The distortion and the tilt are the result of lateral contraction (Poisson’s ratio) and shear deformation (angle γ), though primarily by the latter.

The shear deformation is recognizable by the term in GA . A rigid body rotation over an angle γ is necessary to eliminate the tilt caused by the shear deformation. This rigid body rotation generates an additional displacement at the free end of the beam. This is the contribution of the shear deformation to the deflection. The value of γ is

$$\gamma = \eta \frac{F}{GA}. \quad (2.55)$$

The shape factor η has a value of 1 if the shear stress is constant over the cross-section. For the parabolic variation over a rectangular cross-section the value is 6/5. At the free end of the beam we obtain

$$\varphi = -\frac{1}{2} \frac{Fl^2}{EI} - \gamma, \quad w = \frac{1}{3} \frac{Fl^3}{EI} + \gamma l \quad (2.56)$$

Introduction of γ from Eq. (2.55) and accounting for $A = td$, $I = td^3/12$ and the shear modulus $G = E/2(1 + \nu)$ leads to

$$\varphi = -\frac{1}{2} \frac{Fl}{EI} \left(1 + \frac{\eta(1 + \nu)}{3} \frac{d^2}{l^2} \right), \quad w = \frac{1}{3} \frac{Fl^3}{EI} \left(1 + \frac{\eta(1 + \nu)}{2} \frac{d^2}{l^2} \right) \quad (2.57)$$

The term d^2/l^2 mirrors the influence of slenderness of the beam on the end rotation and deflection. When l/d is larger than five, this term may be neglected. The shear force or shear deformation is not of any importance for slender beams.

Assumption of plane sections

When deriving the classic beam theory, people like Euler and Bernoulli and after them Navier [1] started from the supposition that a plane section normal to the beam axis remains plane and stays normal to the axis. Supposing this, they made no distinction between a constant and linear moment, and found a linear distribution of bending stresses over the depth of the beam. Their finding of the stress distribution is correct, but the membrane theory shows that their supposition holds true only for a constant moment, and that it is at best a good approximation for linear moments in case of slender beams. They were just lucky!

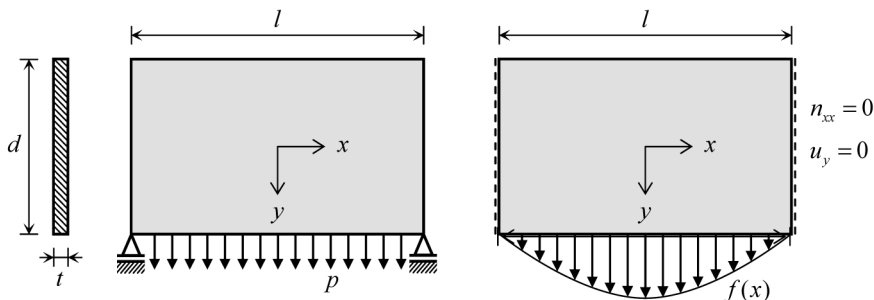


Figure 2.12 Deep beam with edge load.

2.2 Solution for a Wall

Consider a wall on two simple supports for ratios of depth and span ranging from tall wall to slender beam. The wall is loaded along its lower edge by a homogeneously distributed load f , as shown in the left-hand part of Figure 2.12. We want to determine the distribution of the bending stresses σ_{xx} in the vertical axis of symmetry $x = 0$. We replace the structure and load by the problem stated in the right-hand part of Figure 2.12. The supports in the two lower corners have been replaced by boundary conditions for both vertical edges. These edges can freely move horizontally, but prohibit vertical displacements. In the figure this is indicated by the dotted lines. This means that the reaction force will be distributed along the vertical edge. This can be done without changing the bending moment in the vertical cross-section mid-span ($x = 0$). The homogeneously distributed line load f is replaced by a varying load $f(x)$, which has a cosine distribution

$$f(x) = f_m \cos(\alpha x) \quad (2.58)$$

in which $\alpha = \pi/l$ and f_m is the maximum load value at mid-span. This cosine load is the first term in a Fourier series development of load f , so the value of f_m is

$$f_m = \frac{4}{\pi} f \quad (2.59)$$

2.2.1 Beam Intermezzo

We will show that the value of the bending moment M in the mid-span cross-section is practically the same for the actual load p and the replacing load

$f(x)$. The differential equation for beams in bending is

$$EI \frac{d^4 w}{dx^4} = f(x) \quad (2.60)$$

in which EI is the bending stiffness and $f(x)$ is a distributed load. The bending moment M is computed by

$$M = -EI \frac{d^2 w}{dx^2} \quad (2.61)$$

Load f and displacement w are positive if pointing downwards. The bending moment M is positive when tensile stresses are generated in the lower part of the beam. For the homogeneously distributed load, $f(x) = f$. This is a classical case with a well-known solution

$$\begin{aligned} w_{\max} &= \frac{5}{384} \frac{f l^4}{EI} \left(= 0.0130 \frac{f l^4}{EI} \right) \\ M_{\max} &= \frac{1}{8} f l^2 (= 0.125 f l^2) \end{aligned} \quad (2.62)$$

The solution for the cosine load is easily found by substitution of the trial displacement function

$$w(x) = w_m \cos \alpha x \quad (2.63)$$

in the differential equation in combination with the cosine load of Eq. (2.58). This gives us a particular solution

$$\begin{aligned} w(x) &= \frac{f_m l^4}{\pi^4 EI} \cos \alpha x \\ M(x) &= \frac{f_m l^2}{\pi^2} \cos \alpha x \end{aligned} \quad (2.64)$$

Substitution of $f_m = 4f/\pi$ leads to maximum values

$$\begin{aligned} w_m &= \frac{(4f/\pi) l^4}{\pi^4 EI} = 0.0131 \frac{f l^4}{EI} \\ M_m &= \frac{(4f/\pi) l^2}{\pi^2} = 0.129 f l^2 \end{aligned} \quad (2.65)$$

which are close to the correct values shown above. For the cosine load, the proposed shape of the deflection $w(x)$ is the exact one for a beam on simple supports. At the supports, the boundary conditions are $w = 0$ and $M = 0$. These conditions are satisfied, so the particular solution we have found is the real solution. No homogeneous solution needs to be added.

2.2.2 Solution for the Wall

Encouraged by the good result for a beam subjected to a cosine load, we propose a similar cosine displacement field in x -direction for $u_y(x, y)$. This choice meets the conditions that the vertical displacement must be zero at the vertical edges and maximum at mid-span. The horizontal displacement u_x must be zero in the vertical line of symmetry ($x = 0$) and can have values that are not zero (equal, but with an opposite sign) at the two vertical edges. Therefore, we use a sine distribution for u_x . So our expectation for the displacements is

$$\begin{aligned} u_x(x, y) &= u_{xm}(y) \sin \alpha x \\ u_y(x, y) &= u_{ym}(y) \cos \alpha x \end{aligned} \quad (2.66)$$

Here $u_{xm}(y)$ is the distribution of the horizontal displacement along the vertical edges and $u_{ym}(y)$ is the distribution of the vertical displacement along the line of symmetry at mid span. We can choose to work with either $u_{xm}(y)$ or $u_{ym}(y)$. Choosing the former, we substitute the expectation for $u_x(x, y)$ into the bi-harmonic differential equation (2.1), which leads to a normal differential equation for $u_{xm}(y)$

$$\alpha^4 u_{xm} - 2\alpha^2 \frac{d^2 u_{xm}}{dy^2} + \frac{d^4 u_{xm}}{dy^4} = 0 \quad (2.67)$$

We suppose a solution of the form

$$u_{xm} = Ae^{ry} \quad (2.68)$$

Substitution in Eq. (2.67) leads to a characteristic equation for the roots r

$$\alpha^4 - 2\alpha^2 r^2 + r^4 = 0 \quad (2.69)$$

which can be rearranged to

$$(r - \alpha)^2 (r + \alpha)^2 = 0 \quad (2.70)$$

There are two equal roots α and two equal roots $-\alpha$. For equal roots r the general solution has a term with e^{ry} and a term with ye^{ry} . So the solution for $u_{xm}(y)$ becomes

$$u_{xm}(y) = A_1 e^{\alpha y} + A_2 \alpha y e^{\alpha y} + A_3 e^{-\alpha y} + A_4 \alpha y e^{-\alpha y} \quad (2.71)$$

We added a constant α in the second and fourth term in order to give the coefficient A_1 up to and included A_4 equal dimensions. This can be done without loss of generality. Now Eq. (2.2) is used to determine $u_{ym}(y)$. From here on we choose without loss of understanding $v = 0$. Accounting for Eq. (2.2) and after integration, we find

$$u_{ym}(y) = (-A_1 + 3A_2)e^{\alpha y} - A_2\alpha ye^{\alpha y} + (A_3 + 3A_4)e^{-\alpha y} + A_4\alpha ye^{-\alpha y} \quad (2.72)$$

Based on Eqs. (1.9), (2.71) and (2.72) the strains can be expressed in terms of the constants too, and therefore also the membrane forces n_{xx} , n_{yy} and n_{xy} . The four constants then can be determined from four boundary conditions

$$\begin{aligned} y = -d/2 &\rightarrow n_{yy} = 0, & n_{xy} &= 0 \\ y = d/2 &\rightarrow n_{yy} = f_m \cos \alpha x, & n_{xy} &= 0 \end{aligned} \quad (2.73)$$

The elaboration is skipped here. For n_{xx} in the line of symmetry ($x = 0$) we find

$$n_{xx} = \alpha(A_1 e^{\alpha y} + A_2 \alpha y e^{\alpha y} + A_3 e^{-\alpha y} + A_4 \alpha y e^{-\alpha y}) \quad (2.74)$$

Case 1

We consider the case $d/l \gg 1$. This occurs for a tall wall. The stress distribution is highly nonlinear over the depth; in the upper part of the wall the influence of the load on the lower edge is not noticeable, see the left part of Figure 2.13.

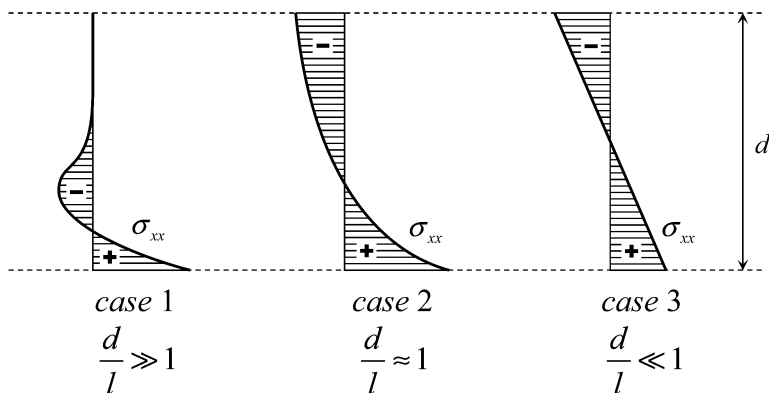


Figure 2.13 Deep beam results for several depth-span ratios.

Case 2

We now consider the case $d/l \approx 1$. This occurs for a wall or beam of which the height and length are nearly equal. The bending stress distribution is again nonlinear over the height, but approaches to classical beam theory. The middle part of Figure 2.13 displays the result.

Case 3

Finally we consider the case $d/l \ll 1$. This is the case for the slender beam and we expect to find the solution for Euler beam theory as drawn in the right-hand part of Figure 2.13. If $d/l \ll 1$, then $\alpha y \ll 1$. For these arguments αy , all the exponential functions can be expanded in a Taylor series around $y = 0$. It appears that the contributions to n_{xx} of powers of αy larger than 1, are negligibly small, so a linear distribution remains. This is the classical solution.

2.2.3 Practical Application

The discussed case of a high wall ($d/l \gg 1$) can be used to estimate the stress distribution in practical structures. An example of this is a silo wall on columns, loaded by a uniformly distributed load, shown in Figure 2.14. This may be its own weight, and wall friction forces due to the bulk material in the silo. To estimate the horizontal stress σ_{xx} in the wall halfway between the columns, we adopt the following approach. The load can be split up into

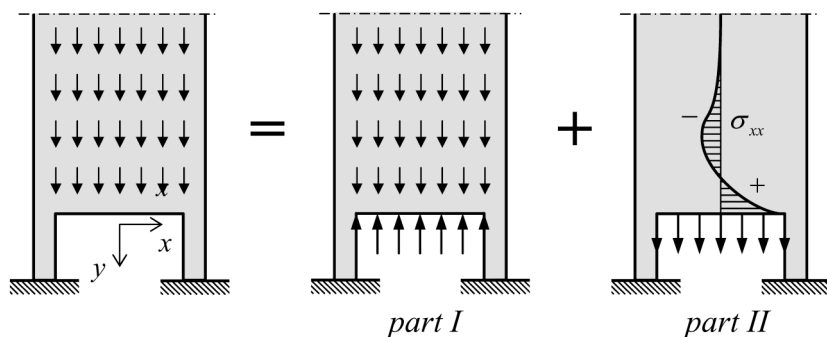


Figure 2.14 Silo wall on columns.

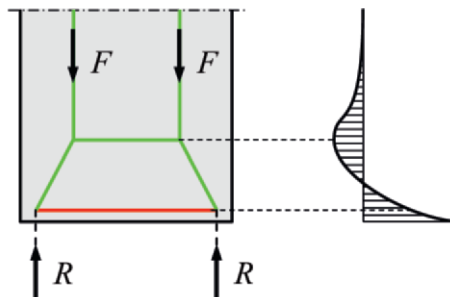


Figure 2.15 Strut-and-tie model for silo wall.

two parts. Part one is a simple stress state in which only vertical stresses σ_{yy} are present and no stresses σ_{xx} occur. We are not interested in this part. The second part is the load case in which the solution for the high wall in Section 2.2.2 can be applied.

Structural engineers who must design reinforced concrete walls often apply truss models for the determination of the reinforcement. For the silo wall they may concentrate the total distributed load in two forces F as shown in Figure 2.15. Each support reaction R is equal to F . The green lines carry compressive forces and the red line the tensile force. The structural engineer wants to know where to place the horizontal compressive strut and the tensile tie, because the distance between them influences the magnitude of the forces in the strut and tie. Knowledge about the elastic solution will be a great help.

2.3 Stresses, Transformations and Principal Stresses

The stresses we have discussed until now have been chosen to be in directions parallel to the x -axis or the y -axis. Sometimes it is useful to know the stresses σ_{nn} , σ_{tt} and σ_{nt} in the directions n and t that make an angle α with the x -axis and y -axis (Figure 2.16). With the help of simple transformation rules, such stresses can be calculated if σ_{xx} , σ_{yy} and σ_{xy} are known

$$\begin{aligned}\sigma_{nn} &= \sigma_{xx} \cos^2 \alpha + \sigma_{yy} \sin^2 \alpha + \sigma_{xy} \sin 2\alpha \\ \sigma_{tt} &= \sigma_{xx} \sin^2 \alpha + \sigma_{yy} \cos^2 \alpha - \sigma_{xy} \sin 2\alpha \\ \sigma_{nt} &= -\frac{1}{2} \sigma_{xx} \sin 2\alpha + \frac{1}{2} \sigma_{yy} \sin 2\alpha + \sigma_{xy} \cos 2\alpha\end{aligned}\tag{2.75}$$

Written in another way

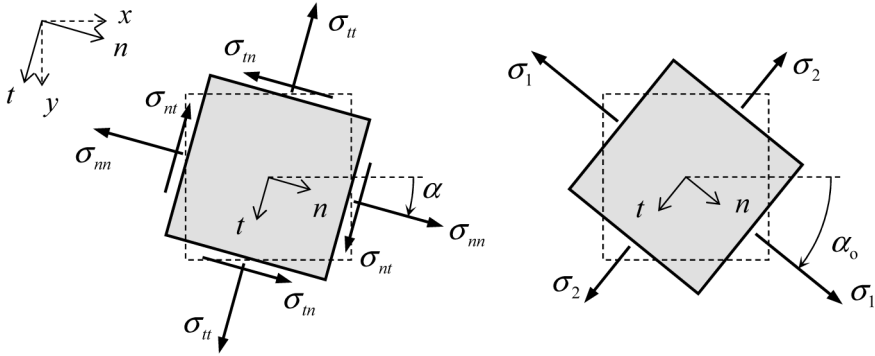


Figure 2.16 Transformation of stresses. Principle stresses and direction.

$$\begin{bmatrix} \sigma_{nn} & \sigma_{nt} \\ \sigma_{nt} & \sigma_{tt} \end{bmatrix} = \begin{bmatrix} \cos \alpha & \sin \alpha \\ -\sin \alpha & \cos \alpha \end{bmatrix} \begin{bmatrix} \sigma_{xx} & \sigma_{xy} \\ \sigma_{xy} & \sigma_{yy} \end{bmatrix} \begin{bmatrix} \cos \alpha & -\sin \alpha \\ \sin \alpha & \cos \alpha \end{bmatrix} \quad (2.76)$$

We see on the basis of Eq. (2.75) that $\sigma_{nn} + \sigma_{tt} = \sigma_{xx} + \sigma_{yy}$. The sum of the normal stresses is invariant under rotations of the axes. An alternative for this transformation is the graphic determination using the Mohr's circle. There is one special value for α that leads to a shear stress value of zero. Then the two normal stresses reach an extreme value. These stresses are called *principal stresses* σ_1 and σ_2 and have the direction α_0 , which is called the *principal stress direction* (Figure 2.16). The principal stresses are

$$\sigma_{1,2} = \frac{\sigma_{xx} + \sigma_{yy}}{2} \pm \sqrt{\left(\frac{\sigma_{xx} - \sigma_{yy}}{2}\right)^2 + \sigma_{xy}^2} \quad (2.77)$$

The direction α_0 belonging to Eq. (2.77) is computed from

$$\tan 2\alpha_0 = \frac{2\sigma_{xy}}{\sigma_{xx} - \sigma_{yy}} \quad (2.78)$$

FE codes may offer the option to show this direction of the principle stresses and refer to it as *trajectories*.

2.4 Other Applications

Consider a circular hole in a plate subjected to a homogenously distributed stress state in which the (normal) stress σ is equal in all directions.

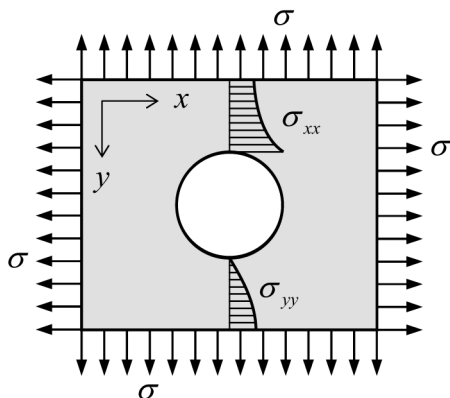


Figure 2.17 Plate with circular hole subjected to a biaxial homogeneous stress state.

The hole causes a disturbance in this homogeneously distributed stress field. Figure 2.17 shows the variation of the stresses σ_{xx} and σ_{yy} along the vertical through the centre of the hole. On the edge of the hole, the stress is: $\sigma_{xx} = 2\sigma$. This means a doubling of the stress of the homogeneously distributed stress state. The factor 2 is called the *stress concentration factor*. We refer to Section 6.1.2 for the derivation.

A higher stress concentration factor occurs at a circular hole in a plate in a uni-axial stress state (see Figure 2.18). At the edge of the hole, a stress of magnitude $\sigma_{xx} = 3\sigma$ can be found.

Another example is a curved beam (see Figure 2.19). The bending stresses in a cross-section no longer vary linearly. In the direction towards the centre of curvature they strongly increase and the maximum stress on the inside may be much larger than can be expected on basis of the elementary bending theory for a straight beam. This is the subject of Section 6.1.3.

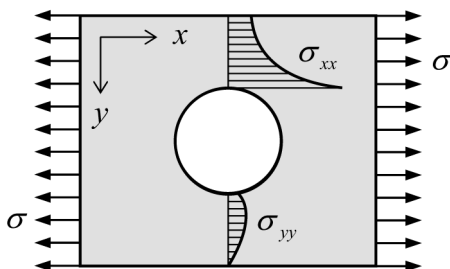


Figure 2.18 Plate with circular hole subjected to a uniaxial homogeneous stress state.

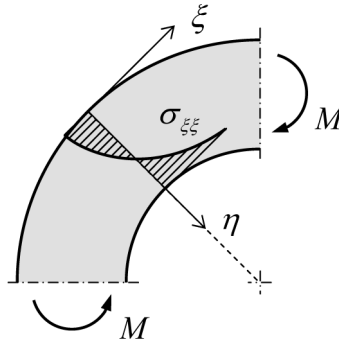


Figure 2.19 Curved bar subjected to a bending moment.

Many interesting stress states can be described with analytical solutions, but many others cannot, for example because the boundary conditions cannot be met or because the contour of the plane stress state cannot be simply described. In such cases numerical methods like the Finite Difference Method or Finite Element Method offer a solution.

We want to give some more examples of stress states that have been determined numerically. First we show another high wall with a load in the middle and restraints along the bottom edge as shown in Figure 2.20. A foundation block can be modeled in this way. The normal stresses σ_{xx} do not vary linearly. The maximum stress at the bottom is noticeably higher than elementary bending theory would have calculated. The moment of these stresses of course should be equal to the total moment in the considered cross-section. Figure 2.20 shows the strut-and-tie model. Green is compression, red is tension.

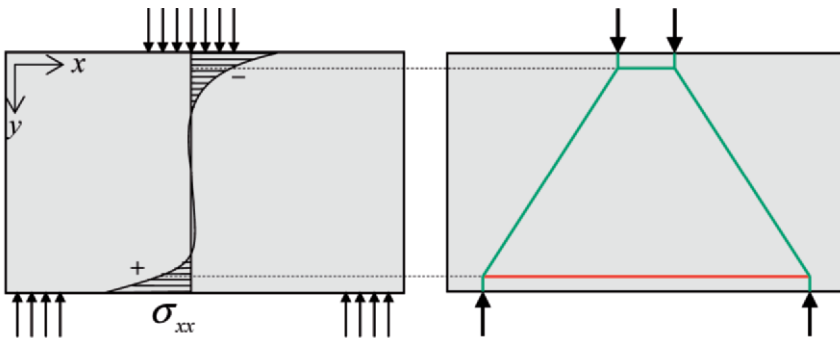


Figure 2.20 Foundation block. Stresses and strut-and-tie scheme.

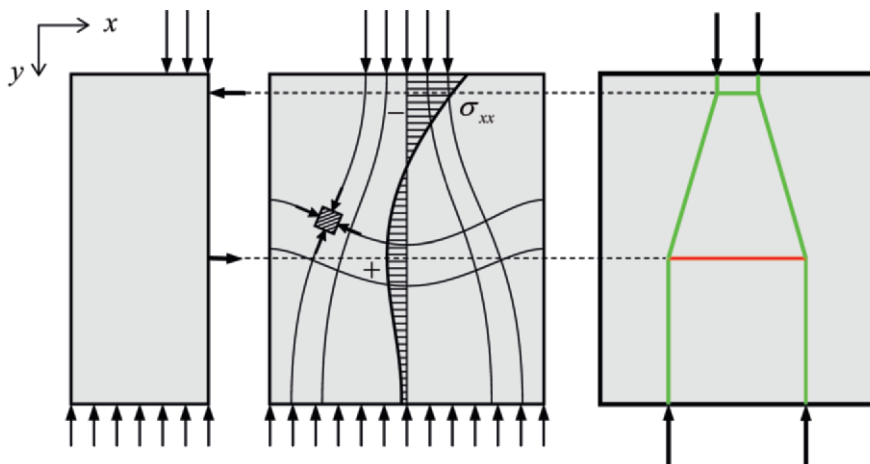


Figure 2.21 Load spreading (for example the anchorage of a pre-stressed cable in a beam).

Another example addresses the load distribution in a beam for the anchorage of a post-tensioned cable. At some distance from the end of the section the forces are distributed uniformly. If we make a vertical cut in the middle and consider one of the halves, then it follows from equilibrium that, in this cutting plane, horizontal stresses σ_{xx} should be present, which are compression stresses at the top and tensile stresses at some distance from the top. The distribution shows the attenuated character again. Practice is not ordinarily prepared for these tensile stresses. They can lead to cracks in the plane of the beam axis; a concrete beam will require reinforcement in the form of stirrups or spiral reinforcement. Figure 2.21 shows some principal stress trajectories. The corresponding strut-and-tie model is also shown.

A similar example of load spreading is the foundation footing, as found under buildings with brick walls (see Figure 2.22). If we make another vertical cut and consider the equilibrium of one of the halves, it will show the presence of horizontal tensile stresses σ_{xx} at the bottom. To determine the magnitude, the stress problem has to be fully solved. The broader the base of the foundation, the lower is the pressure on the soil. However, the tensile stresses in the brickwork will increase, and the poor tensile strength of this material will soon lead to cracks.

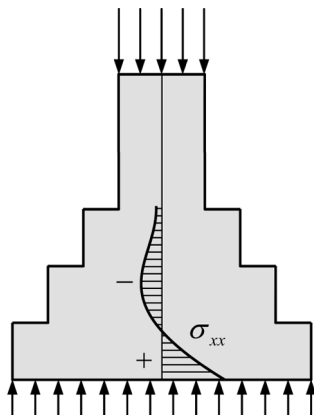


Figure 2.22 Foundation foot. Stresses and strut-and-tie scheme.

Set-back corners (window, door or other openings in a wall) deserve special attention. Figures 2.23 and 2.24 give two more examples. If there is no rounding in the corner the stresses are theoretically infinitely large. In this relation we speak of *notch stresses*. Many cracks are the result of this, and many accidents have occurred (e.g. airplane industry). These corners need special attention from the designer. Often the corners have to be rounded off (plane windows) or strengthened in another way. Concrete structures need special detailed designs for the reinforcement in such corners.

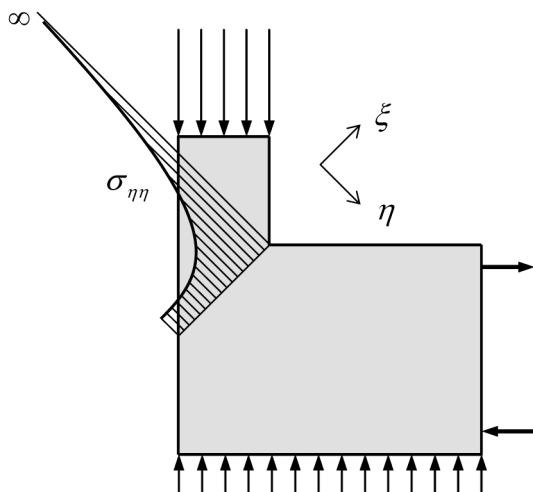


Figure 2.23 Set-back corner.

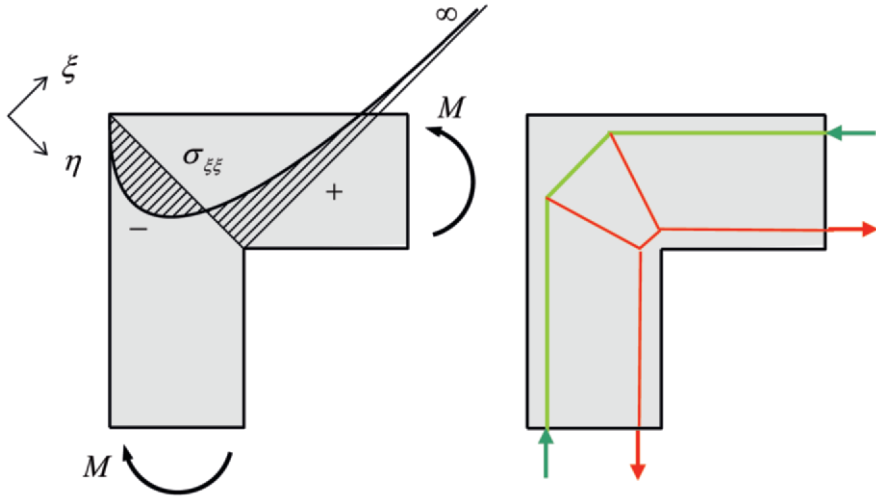


Figure 2.24 Beam-column connection. Stresses and strut-and-tie scheme.

2.5 Message of the Chapter

- One stress state can correspond to more than one displacement field; the difference between the fields are rigid body motions, displacement fields with zero strains. A rigid body motion leaves the structure stress-less.
- Displacements due to a constant bending moment in classical bending theory for a beam of thin cross-section are confirmed by the plane stress membrane theory. Plane sections before loading remain plane after loading. The well-known simple formulas for the deflection and rotation in basic standard cases are confirmed.
- The membrane solution for a constant shear force, in combination with a linearly varying bending moment, deviates from classical beam theory. Plane sections are no longer plane after loading. A linear distribution of bending stresses over the depth of the beam is accompanied by a distorted cross-section. The simple formulas for deflection and rotation in classical beam theory must be amended

for shear deformation. This amendment is negligible if the cantilever length is over five times the beam depth.

- The distribution of bending stresses in a shear wall is dependent on the ratio of the wall depth and span. Three aspect ratios are considered. For a high ratio (tall wall) the bending stress distribution is highly nonlinear, and the top part of the wall does not contribute to the load transfer. For a ratio in the order of unity (square wall) the distribution is still nonlinear, but the full cross-section participates in the transfer. For a low ratio (slender beam) the stress distribution approaches to the linear distribution of bending stress in classical beam theory.
- From the computed stress state we can compute two principal stresses and their direction. Trajectories are an instructive and insight-providing aid to structural designers.

Plates and FEM

Surprises and Pitfalls

Blaauwendraad, J.

2010, XXVI, 414 p., Hardcover

ISBN: 978-90-481-3595-0